DOI: XXX-XXX-XXXX

Optimal number of control points for fitting B-splines in Wind Turbine Blade Measurement

Ching Hin Lydia Chan[1], Qing Wang[1#], Roger Holden[2], Songling Huang[3] and Wei Zhao[3]

1 Department of Engineering, Durham University, DH1 3LE, UK
2 Nikon Metrology UK Ltd, Castle Donington, Derby, DE74 2SA, U.K.
3 Department of Electrical Engineering, Tsinghua University, Beijing 100084, P. R. China
Corresponding Author / E-mail: qing.wang@durham.ac.uk, TEL: +44-191-334-2381, FAX: +44-191-334-2408

KEYWORDS : Coherent laser radar, 3D metrology, B-spline fitting, data alignment, large-scale manufacture inspection

The manufacture of large-scale products such as aircraft and wind turbines needs detailed inspection to ensure the required dimensional tolerances are met. A Coherent Laser Radar with an assisting mirror was used in this research to inspect a half-size wind turbine blade. This paper investigates the optimal distribution of inspection points that would produce the most accurate B-Spline fitting to the CAD model surfaces and so shorten the inspection and analysis process without compromising on accuracy. Even though the optimal solution was found to be points with 100mm spacing on a moderate surface gradient and with 20-25mm spacing on a more severe surface gradient, the findings suggest the employment of a non-uniform distribution would produce a more accurate fitting. This paper also explores data alignment by Degree of Freedom (DoF) constraints with a triple B-Spline and investigates whether denser data points would improve the transformation. The optimal solution was found to be constraining movement in Z, Rx and Ry. Therefore, to achieve better transformation, surfaces were treated based on their gradient. This resulted in a constraint in X, Y and Z, and Ry for a moderate gradient and Y, Z and Rz for a more severe gradient. The optimal number of inspection points for fitting a B-Spline on a half-size blade was found to be 18 points for the front section with 100mm spacing, 15 points for the back section with 100mm spacing, and between 14 and 18 points with 20-25mm spacing on the base section.

Manuscript received: August XX, 201X / Accepted: August XX, 201X

1. Introduction

There is an increasing demand for suitable measurement systems to be used in large-scale manufacturing industries such as aerospace, shipbuilding, automotive, and power generation equipment. Metrology instruments are known to be highly flexible, reliable, and capable of aiding manufacturing tasks from production to final inspection.

Many large-scale metrology techniques have been reviewed since computational technologies began their exponential growth. Puttock, [1], Estler et. al. [2], Peggs et. al. [3] Franceschini [4] and Schmitt et al [5] have surveyed a variety of metrology techniques from different perspectives over the years. Accuracy and accessibility are key to choosing a suitable system for the task [6]. Weckenmann et. al. [7] described the advantages, challenges and scope in the application of multi-sensors in dimensional metrology. Galetto and Parlio [8] investigated the positioning of ultrasonic beacons as sensors in large-scale metrology applications and developed an algorithm that improved their placement compared to existing practices. Ramasamy and Raja [9] assessed the performance of different multi-scale data fusion methods and identified Regional Edge Intensity (REI) as the preferred method for measuring engineered surfaces. Galetto et. al. [10] presented a way of fusing distributed multi-sensor large volume metrology (LVM) systems that combines the angular and distance readings of each system's sensors. In contrast, Maisano and Mastrogiacomo [11] proposed a methodology that uses only angular measurements to create multi-sensor networks of devices for distributed large-volume metrology systems. Franceschini et. al [12] developed Galetto et al's technique further by comparing competitive and cooperative data fusion using a combination of multiple LVM systems and various types of sensors. Galetto et. al. [13] introduced a new method for estimating uncertainty in relation to locating specific targets in distributed large-scale metrology systems that incorporates the Monte Carlo method. Jang and Kim [14] reviewed the progress made on the compensation of the refractive index of air in order to improve the measurement uncertainty of laser-based distance measurements. Jian Wang et. al. [15] studied four types of weighted fusion methods and concluded that they formed a useful system for measuring freeform surfaces. M. J. Ren et. al. [16] then developed and verified a robust weighted least square-based data fusion method for multi-sensor measurements of complex surfaces.

Products in large-scale manufacturing industry are generally very

large in dimension and require high precision production. Hence, they must be inspected in detail to ensure the tight geometric tolerances are satisfied. Many of these products, for example, wind turbine blades and aircraft wings, are manufactured based on computer-aided design (CAD) models and contain complex freeform surfaces. The inspection technique would largely be based on the comparison between the theoretical model and the actual product. Metrology systems enable measurements to be taken from the actual product and comparisons to be made via compatible software using the data points [17] [18].

In this research, a Coherent Laser Radar with an assisting mirror was used to investigate B-Spline fitting points and data alignment to CAD on a half-size wind turbine blade with freeform surfaces. The objectives were as follows:

1. The inspection duration is dependent on how many points on the object are in query. The amount would affect the fitting of B-Splines on freeform surfaces. The investigation aims to find the minimum number of points to be measured for data alignment that would be sufficient to provide a good B-Spline fit. The time taken for measurements and, hence, the inspection time could therefore be reduced.
2. A previous study has been carried out using single and double B-Splines to find the optimal DoF constraint data alignment on freeform surfaces [19]. In order to investigate how closely the located data points would affect the transformation, a triple B-Spline with tight-fitted points on the curves will be used to test and evaluate the 32 variations in DoF constraints on data alignment on the freeform surfaces to identify the optimal solution. Results will be compared to the previous study to establish any correlation [20, 21].

2. Metrology Theory

2.1 Coherent Laser Radar (CLR)

Coherent Laser Radar (CLR) technology [22] is used as an optical scanning technique to provide fast and accurate measurements. A linear optical signal is emitted by a frequency modulated infrared laser diode, and the return detection would only need to be about 1% of the reflected beam from the target to determine the measurement. The returned beam is then coherently mixed with the transmitted signal to produce a beat frequency, Δf, which is proportional to the range, R, and can be determined by:

$$R = \frac{c\ t\ \Delta f}{2\ (f_{max} - f_{min})} \qquad (1)$$

Where c is the speed of light, t is the time taken for the frequency to reach from f_{min} to f_{max}, f_{max} is the amplitude of the frequency wave form, with a typical value of 200THz, and f_{min} is the base frequency, which has a typical value of 100GHz [3].

Nikon Metrology's FM CLR Scanner (model MV200) was used in this research [23]. The laser beam is steered precisely by a scan mirror that is mounted on a two-axis gimbal, as shown in Figure 3. The instrument is capable of scanning at a range (*Rg*) of up to 50m to a resolution of 1μm. It can be controlled through 360° in Azimuth (*Az*) and 120° in Elevation (*El*) to a resolution of 0.33 asec. The general mechanism is illustrated in Figure 1. For a target point that is 2m away, the instrument can measure with a 3D uncertainty of 24μm. By combining the Azimuth and Elevation angles, with the range calculated with the beat frequency, the measured point can be located and converted into Cartesian coordinates via the accompanying software.

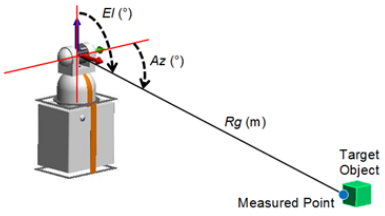

Fig. 1 CLR scanner measuring principles

2.3 Software Compatibility

The software chosen for this research is Spatial Analyzer (SA) by New River Kinematics. It is a flexible, instrument-dependent and traceable 3D graphical software platform that is designed for large-scale manufacturing applications [24]. SA is capable of accommodating any number of metrology instruments of any type simultaneously and collating data into a single coordinate system.

In this research, SA is used to control the Laser Radar and take measurements at a pre-planned set of inspection points on the piece based on its CAD model. The data is then manipulated through a 'Relationship Fitting' process to optimise the alignment between the measured and the nominal reference. This best-fit transformation utilises the Least Square method, which is a standard approach to the approximate solution of over-determined systems in adjusting the parameters of a model function to best fit a data set. The transformation works by altering combinations of DoF constraints, that is, to constrain transformation movement in a variation along Cartesian axes, X, Y and Z, or rotate about these three axes (denoted by Rx, Ry and Rz).

There are other software on the market that do the same as SA. The main difference is the design origin of these programs. Other available software, such as PolyWorks by InnovMetric and Metrolog X4 by Metrologic Group, are based on point cloud treatment and the analysis of measured data from individual instruments, whereas Verisurf by Verisurf Inc. provides interoperability between CAD models and instruments.

2.4 Generating Inspection Points on B-Spline curves

A B-Spline is a piecewise polynomial function and can be generated using de Boor's algorithm [25]. An approximate curve can be defined by:

$$C(t) = \sum_{i=0}^{n} P_i\ N_{i,k}(t) \qquad (2)$$

Where Pi is the i-th control point, N(t) is the basis function, and k is the order of polynomial segments.

In SA, B-Splines are generated by intersecting a predefined plane in the Z-direction with the CAD surfaces and combing together for each surface section using knot adjustment [26] [21]. Inspection points

DOI: XXX-XXX-XXXX

are then created along each B-Spline to mark where measurements are to be taken. These points would be measured automatically in groups according to the B-Splines via the SA command.

A Hausdorff distance, as shown in Figure 2, would be produced between the exact CAD surface B-Spline and the generated B-Spline [27] [28]. Therefore, all created inspection points must be projected to the exact CAD surfaces to reduce the error associated with B-Spline approximation.

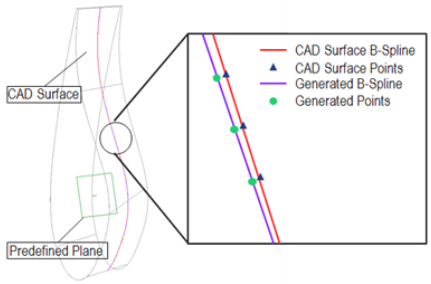

Fig. 2 Hausdorff distance between exact CAD B-spline and approximated B-Spline

The number of points created is proportional not only to accuracy but also to the inspection and processing time. Hence, it is important to allow a sufficient number of points to be generated to give the most accurate B-Spline representation that requires the least time to measure and for the data to be processed [29][30].

3. Measurement Method

3.1 Experiment Setup and Equipment

Experiments were performed on a half-sized cross-section model of a wind turbine blade. The test piece was based on the Vesta 44m offshore wind turbine blade at 5.5m from the root. The test piece is 1.65m in height and 0.5m in width. The blade is divided into three sections – front, base and back – to represent freeform surfaces of different curvature. The piece was mounted on a gimbal and turntable to allow rotation along the three Cartesian axes – X, Y and Z. Different blade flex scenarios of sag and twist can be replicated by adjusting the two to the nearest degree.

The Laser Radar was placed about 2.5m away from the test piece in the laboratory. Five tooling balls were placed on the side of the test piece for setting up alignment between the LR and the CAD model in SA. The change of instrument position was simulated by rotating the turntable, instead of moving its location, to avoid damaging or entangling the connections. This would also help maximize measurement accuracy by minimising misalignment.

For places on the test piece where the Laser Radar could not measure directly (e.g. the base), a micron-polished nickel-plated aluminium mirror of 15cm diameter was employed. The optic beam travels from the LR to the mirror and is reflected onto the test piece. A tooling ball was used to align the mirror view to the LR and a mirror plane was created on SA with the reflected data. Even though the mirror provided access to a restricted view area, it is very small, so to measure all the inspection points requires constant readjustment to a new view, which is very time-consuming. The test piece was raised ~20cm above the bench for a clearer mirror view. The mirror was also kept under a 50° incident angle to ensure confident measurements. The test piece and mirror setup are shown in Figure 3.

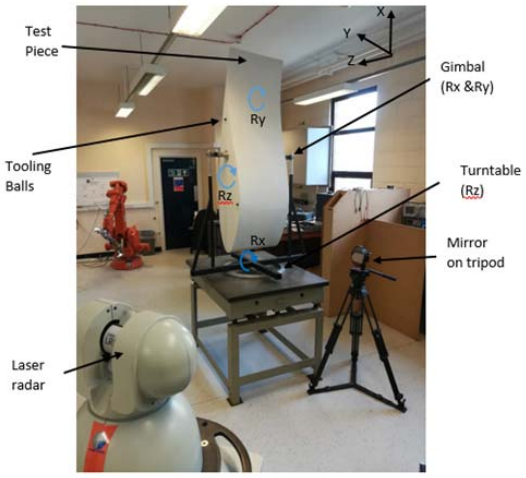

Fig. 3 Half-sized cross-section wind turbine blade test piece on a gimbal and turntable with the assisting mirror

3.2 Experiment Plan

Two experiments were designed to investigate the objectives:

Experiment 1 – The number of inspection points on a single B-Spline at the centre of the blade were varied. The data points were then transformed using Nikon Metrology's current alignment technique – Z, Rx and Ry constraints. A new B-Spline was then mapped through these points and compared to the nominal points on CAD for any deviation.

Experiment 2 – Three B-Splines were evenly constructed along the blade surfaces at 125mm, 250mm and 375mm (as shown in Figure 4). Inspection points were spread 25mm apart at the front and back section, and 10mm apart at the base. The number of points were 69, 35 and 60, respectively. Two blade flex scenarios were used: Offset 1 – 0°Rx, 0°Ry, 0°Rz (No flex); and Offset 2 – 30°Rx, 5°Ry, 10°Rz (most extreme flex).

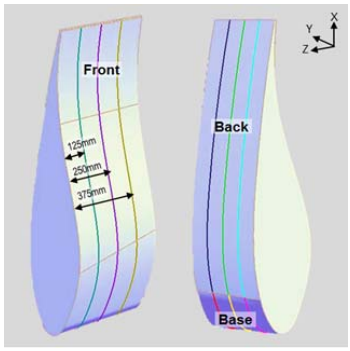

Fig. 4 Experiment 2 triple B-Spline arrangement

The data collection procedure developed by Nikon Metrology was implemented in the designed experiments as it is commonly used in large-scale manufacturing and considered to be reliable. The process is illustrated in Figure 5:

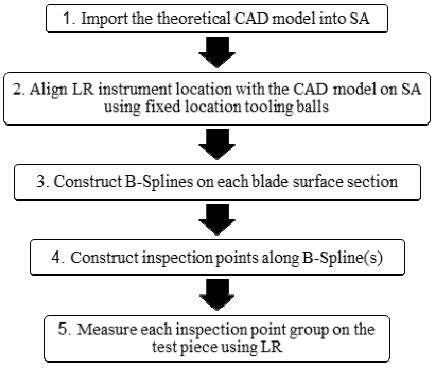

Fig. 5 Data collection procedure

Once all inspection points have been measured, data transformation can begin. Firstly, the distance between the raw data and the CAD surfaces is reduced by rotating about the datum in the selected DoF. The point-to-point distance between the raw data and the equivalent CAD inspection point is also minimised. Transformation was only carried out once with the stated constraints for Experiment 1, whereas in Experiment 2 raw data were duplicated and the transformation was repeated for the 32 DoF combinations.

3.3 Analysis Criteria

Transformed data were exported and analysed. For Experiment 1, the coordinates of the transformed data points were compared with the nominal. Any deviations were noted and examined.

For Experiment 2, the data was analysed following these three criteria:

Point-to-CAD Surface Distance – this measures how far away the transformed points on each B-Spline are to the CAD surfaces. The mean and variance of the distance were calculated and compared against ones on the other blade section. The smallest values represent the closest alignment towards the CAD surfaces and hence the optimal and most accurate DoF constraints combination.

Point-to-Nominal Point Distance – the mean and variance of the distance between the transformed points on each B-Spline and the corresponding nominal point were quantified. The smallest values represent the least deviation from the original and hence the optimal and most accurate DoF constraints combination.

Instrument Movement – this measures the mean and variance of the distance at each DoF constraint from the transformed instrument location to the original reference frame, which is also the fully constrained DoF (X, Y, Z, Rx, Ry and Rz). The least movement represents the optimal and most accurate DoF constraints combination.

Each set of data was compiled and a ranking system was used to compare each DoF constraint variation. Based on the three analysis criteria above, the results were ordered based on each category from smallest to largest and given a score from 1 to 32 depending on their rank. The summation of all three scores, which is point-to-CAD surface distance, point-to-nominal point distance and instrument movement, provided an overall ranking, which could lie between 3 and 96. The DoF constraints in combination with the lowest overall score would indicate the best performance throughout and would therefore be the optimal solution.

4. Results and Analysis

All values are presented in millimetres (mm) and rounded to the nearest 0.01mm based on the implemented measurement method used in SA.

4.1 Experiment 1 – Point Investigation

The fitting of a single B-Spline with a varying number of points was evaluated in this experiment. From the research by Li et al. [35], it was suggested that a total of 90 points would obtain the minimum value of deviation when defining an aerofoil with a B-Spline. Therefore, this experiment would examine B-Spline fitting around this finding.

Front blade section – the difference between the measured B-Spline and the nominal was compared based on the number of inspection points, which were generated in 25mm increments. This resulted in creating 69, 35, 18, 14 and 12 points along the B-Spline with 25mm, 50mm, 100mm, 125mm and 150mm spacing, respectively. The findings are illustrated in Figure 6.

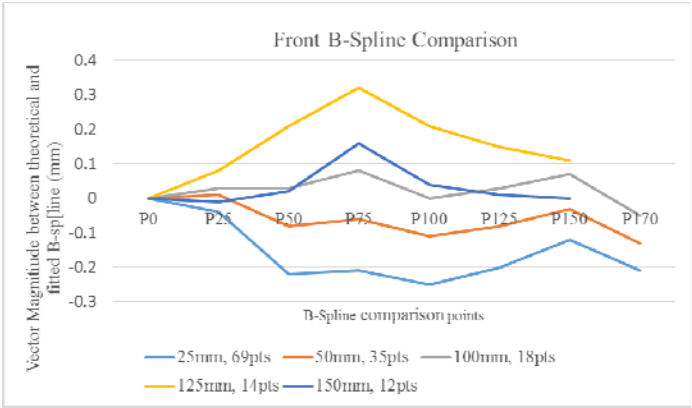

Fig. 6 Front B-Spline fitting comparison with a varying number of points

Measuring with 14 points in the front section showed the highest deviation whereas the smallest was shown with 18 inspection points. In general, there is a parabolic pattern in the relationship between the number of points in this section and the difference in location. Therefore, the optimal spacing is found to be 100mm on the front section of a half-size blade.

Base blade section – The inspection points were constructed in 5mm increments as the curvature in this section is more extreme. This resulted in creating 35, 24, 18, 14 and 12 points along the B-Spline with 10mm, 15mm, 20mm, 25mm and 30mm spacing, respectively. The findings are illustrated in Figure 7.

DOI: XXX-XXX-XXXX

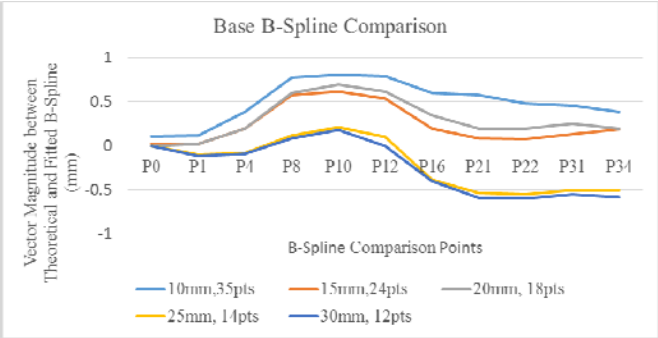

Fig. 7 Base B-Spline fitting comparison with a varying number of points

With a different curvature profile in this section, the relationship between the number of points and the B-Spline fitting appeared to be more linear than parabolic. There is a smaller difference in the first section of the graph (left half of Figure 7), and as the measurement progresses further along the section the difference appears to increase (right half of Figure 7). The optimal spacing appears to be between 20mm (18 points) and 25mm (14 points) on the base section of a half-size blade.

Back blade section – Similar to the front blade section, the inspection points were generated in 25mm increments. This resulted in creating 60, 30, 15, 12 and 10 points along the B-Spline with 25mm, 50mm, 100mm, 125mm and 150mm spacing, respectively. The results are illustrated in Figure 8.

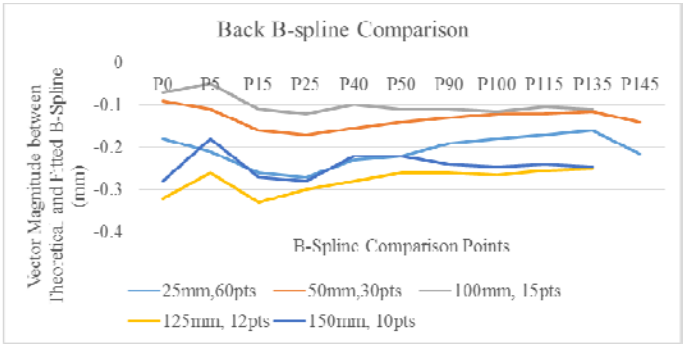

Fig. 8 Back B-Spline fitting comparison with a varying number of points

The effect of varying the number of inspection points appears to be the same as for the front blade section – there is a parabolic relationship as the number increases. The optimal point spacing was found to be 100mm with 15 points in total on the back section of a half-size blade.

Table 1 shows the inspection times used for each different number of inspection points constructed on the front, base and back sections of the blade. The minimum times are for 18 points on the front, 14 points on the base and 15 points on the back, which broadly agrees with the number of inspection points for optimal point spacing.

Table 1: Relations between inspection points and inspection time

Front		Base		Back	
Points	**Inspection time (mins)**	**Points**	**Inspection time (mins)**	**Points**	**Inspection time (mins)**
69	20	35	38	60	24
35	11	24	30	30	15
18	8	18	25	15	10
14	9	14	24	12	14
12	10	12	26	10	16

4.2 Experiment 2 – Triple B-Spline transformation

Offset 1 – Measurement simulating a blade flex of 0°Rx, 0°Ry, 0°Rz (No flex) using triple B-Spline on blade surfaces

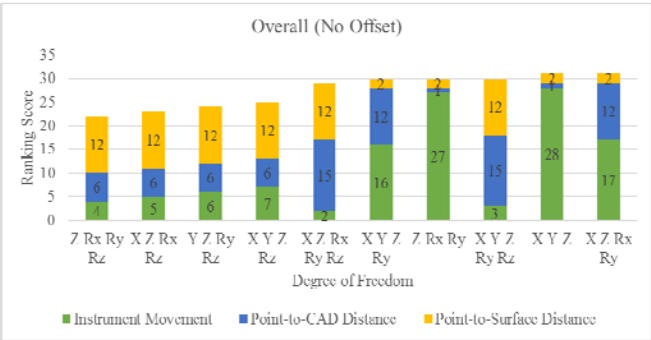

Fig. 9 Offset 1: DOF Constraints transformation ranking score results

Table 2: Offset 1 – Top 10 ranking score results

DoF	Point-to-Surface	Point-to-Point	Instrument Movement	Total Score	Over all Rank
Z Rx Ry Rz	0.95	1.06	1.46	22	1
X Z Rx Rz	0.95	1.06	1.48	23	2
Y Z Ry Rz	0.95	1.06	1.54	24	3
X Y Z Rz	0.95	1.06	1.55	25	4
X Z Rx Ry Rz	0.95	1.11	1.35	29	5
X Y Z Ry	0.94	1.08	5.07	30	6
Z Rx Ry	0.94	1.04	14.43	30	6
X Y Z Ry Rz	0.95	1.11	1.44	30	6
X Y Z	0.94	1.04	14.50	31	9
X Z Rx Ry	0.94	1.08	5.11	31	9

There is a clear variation between the higher and lower ranked DoF in their total scores, as shown in Figure 9 and Table 2. However, when looking at the actual values of Point-to-CAD Surface distance, Point-to-Nominal Point distance, and Instrument movement, the numerical variance is very small – only a maximum of 0.2mm difference in the top 5. All of the top 10 constraints have very low

scores in the three criteria.

The optimal DoF data alignment solution in this part of the experiment was achieved through a Z, Rx, Ry, Rz constrained transformation, allowing movement in X and Y. It gained an overall score of 22. However, there is only a 0.02mm difference in instrument movement distinguishing it from the second ranked (X, Z, Rx, Rz constraints).

Offset 2 – Measurement simulating a blade flex of 30°Rx, 5°Ry, 10°Rz (No flex) using triple B-Spline on blade surfaces

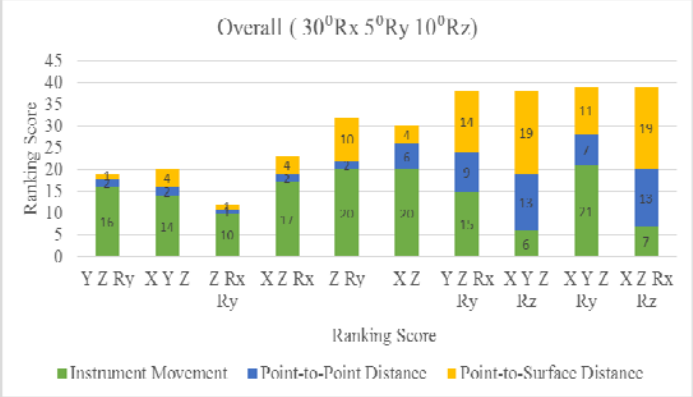

Fig. 10 Offset 2: DOF Constraints transformation ranking score results

Table 3: Offset 2 – Top 10 ranking score results

DoF	Point-to-Surface	Point-to-Point	Instrument Movement	Total Score	Overall Rank
Y Z Ry	1.11	1.46	9.43	19	1
X Y Z	1.12	1.46	9.24	20	2
Z Rx Ry	1.11	1.45	9.69	20	2
X Z Rx	1.12	1.46	9.44	23	4
Z Ry	1.30	1.46	12.36	32	5
X Z	1.12	1.58	22.36	38	6
Y Z Rx Ry	1.43	1.75	9.34	38	6
X Y Z Rz	1.55	1.86	4.90	38	6
X Y Z Ry	1.39	1.60	14.81	39	9
X Z Rx Rz	1.55	1.86	5.06	39	9

The variation in the ranking score is more gradual with this offset and the difference in the top 10 is more distinct, as shown in Figure 10 and Table 3. Even though there are larger instrument movements when compared to Offset 1, the difference in Point-to-CAD Surface and Point-to-Nominal Point distances are below 0.01mm among the top ranked DoF with a total score under 23.

The Y, Z, Ry constrained transformation gained the lowest score of 19 in the ranking and therefore is the optimal alignment solution in this part of the experiment. Again, there is still a very small numerical difference distinguishing the top 3.

5. Discussion

5.1 Experiment 1 – Points Investigation

Overall, inspection points with 100mm spacing achieved the least difference in fitting measured points to the nominal B-Spline for the front and back blade sections using 18 and 15 points, respectively. Even though this spacing gave the most accurate results, there still appears to be a moderate amount of difference in both sections, especially at the back. This is thought to be induced by the changing of instrument location for measurement. Without a 100% certain alignment between the CAD model and LR, it will always inherit an offset from the movement. In this experiment, due to laboratory conditions the instrument relocation could only be simulated by spinning the test piece with the turntable so that the relative location between the two is produced. However, for industrial applications, the instrument can be physically relocated and aligned with another dedicated set of tooling balls, which could minimise the chance of misalignment. Instead of placing tooling balls on the blade, they can be fixed in the surrounding area. Any instrument relocation can be calibrated with respect to the environment and the test piece can remain stationary, which could reduce misalignment.

As shown in Figure 7, all inspection point variations experienced a peak with the fitting difference in the central area at the front blade section. Since the test piece is an aerofoil, that particular area experiences a more dramatic curvature, as displayed in Figure 4. It is the nature of B-Spline fitting to have denser points when mapping more complex curves [41]. Therefore, rather than having evenly distributed points along the front B-Spline, closer points might be needed for that area.

Similarly, in the base section, the B-Spline has different curvature profiles across, producing fluctuating results, as shown in Figure 8. The use of a mirror could have possibly made a contribution to the variance in the overall results due to misconfiguration with the measuring mirrored plane. However, it would be hard to eradicate this situation as it is part of the instrument design. Nonetheless, the best fitting was achieved by a 15mm spacing of inspection points in general, even though there was still a certain amount of deviation throughout. Again, an irregular spread of inspection points could help minimise the difference.

Having found the optimal spacing for a half-size blade, fewer points are needed to be measured in the inspection process. With confidence in a sufficient number of inspection points, B-Splines can be mapped accurately and efficiently so that measuring and process time can be reduced.

5.2 Experiment 2 – Triple B-Spline points transformation

The two blade offsets applied in this experiment achieved different optimal DoF constrained transformations. Z, Rx, Ry and Rz constraints were the optimal for no flex (Offset 1) and Y, Z and Ry constraints were the optimal for the most extreme flex scenario (Offset 2). Results were extracted as an average across all blade surfaces. However, Z, Rx and Ry (Nikon's current technique) came top among the combination of both offsets.

With a triple B-Spline transformation, points were located closely, which improved the overall accuracy and achieved very small Point-to-CAD Surface distances, Point-to-Nominal Point distances, and Instrument movements, throughout. This also provided more coverage across the blade so a larger surface could be measured in detail. Given the three criteria attained very close transformation results, factoring

DOI: XXX-XXX-XXXX

the instrument uncertainty made it very hard to distinguish which DoF constraints among the top few provided the best alignment. Hence, it is important to know the tolerance of the part being measured. A triple B-Spline transformation can also provide alignment for tight specifications since it has the ability of achieving a near accurate alignment.

When analysing results for individual surfaces, the optimal transformations for each blade section are given in Table 4:

Table 4: Optimal DoF constraints transformation for individual blade sections

Blade Section	Optimal DoF	Offset 1 Score	Offset 2 Score	Total Score
Front	X Z Rx	3	2	5
Front	X Y Z Ry	2	3	5
Base	Y Z Rz	1	1	2
Back	X Y Z Ry	2	6	8
Back	X Z Rx Ry	1	7	8

As the previous study suggested [23], Y, Z and Ry constraints did achieve optimal results in Offset 2 overall and, as the back section alone, also remained in the top 10 in all sections for both offsets. However, their rankings within Offset 1 were at the lower end. This could partly be due to misalignment of the test piece as the tooling balls had less difference in Elevation and Azimuth. This could also relate to the individual operator's technique in alignment, measurement, or using the mirror.

Even though the newly suggested constraints of Y, Z and Ry were ranked top when the offset was at its most extreme, this raised the question of whether different offset scenarios and blade sections require separate transformation constraints. If each blade section was treated separately, better alignment could be provided and a closer fit could be achieved. Each section could be overlapped to avoid intermediate gaps and provide a certain degree of interaction amongst them to still treat them as a complete blade. Therefore, deriving from experimental results, the following DoF constraint transformations are suggested for each section of the blade (Table 5):

Table 5: Suggested DoF constraints transformations for each section across the blade

Surface Section	Suggested DoF
Front	X Y Z Ry
Base	Y Z Rz
Back	X Y Z Ry

5.3 Experiment Technique Evaluation

Instrument calibration is an important element for providing reliable measurements. The LR used in the experiments was of an older generation and has not been serviced recently. Despite carrying out quick setup tests before taking each set of measurements, it is possible that some calibration error has been inherited due to the lack of servicing.

Alignment with tooling balls would also affect measurement results. This is mostly due to the focus of the beam on the tooling ball where false alignment can be produced by not pointing the beam at the focal spot on the tooling ball. Techniques in such must be addressed to avoid introducing error in test measurements.

When it comes to using a mirror to aid the measurement of the base blade section, it is important to ensure the mirror is placed at a small incidence angle. This would ease the tooling ball alignment process and measurement confidence. It was found that placing the mirror on the right and close to the bench provided the easiest tooling ball alignment and measurement angle in laboratory conditions (illustrated in Figure 11). It was able to cover a good number of inspection points for each measurement period.

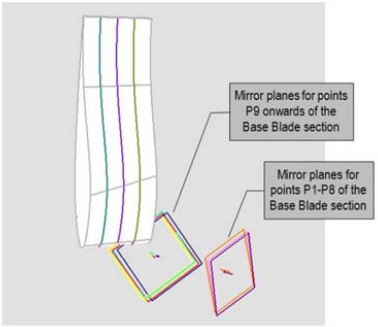

Fig. 11: Mirror plane used in both experiments for measuring the base blade section

Despite easing the measurement process, it was very time-consuming to move the mirror on the tripod to a new location for each cluster of points. Though the tripod provided sturdy support, its restricted mobility means that it is sometimes difficult or impossible to provide a suitable location for the mirror plane. Instead of a fixed base tripod, an extension arm or even a robotic arm could be used to offer a smoother mirror relocation process.

6. Conclusion

Experimental results showed that the optimal number of inspection points for fitting a B-Spline on a half-size blade was found to be 18 points for the front section with 100mm spacing, 15 points for the back section with 100mm spacing, and between 14 and 18 points with 20-25mm spacing on the base section. Based on the nature of B-Spline fitting, a non-uniform spread of points has been suggested, as sections with more complex curvature require more points compared to straighter curves. Recommendations were made to create tighter points in the mid-front and the earlier base sections, and slightly fewer in the later base sections.

The investigation also found that a triple B-Spline transformation provided more accurate alignment results with some analysis criteria values locating near the 1mm mark. The overall optimal alignment solution was found to be Z, Rx and Ry constraints as Nikon Metrology has suggested. However, different solutions were found when sectioning the blade surfaces based on the B-Spline curvature. Therefore, a proposal was made to treat each blade section separately for data alignment by maintaining an overlap to keep the relationship as a whole blade. The individual blade section could receive a different tolerance according to the design specification and data

alignment could be performed separately to provide a better fit. A set of DoF constraints was suggested as follows: Front and Back – X, Y, Z and Ry; Base – Y, Z and Rz.

The measurement technique was also reviewed. Due to lack of maintenance, it is possible that the LR has induced a larger instrument uncertainty than expected. Also, when aligning the instrument to the CAD model, the focal point on each tooling ball must be located precisely in order to avoid additional error in the measurement. Furthermore, ideal placement of the mirror to measure the base blade section was recommended based on laboratory conditions. Rather than using a tripod to hoist the mirror, it has been suggested to use an extension arm or robotic arm for a smoother transition when relocating the mirror to a new measurement angle.

Despite using a half-size cross-section wind turbine blade in this investigation, the same technique can be used in other large-scale manufacturing inspection processes, such as aircraft body or vehicle production. With sets of well-mapped B-Spline inspection points, measurements can be taken efficiently and accurately for CAD model comparison. The suggested alignment solution can also be applied and selected based on similar curvature profiles as that of the turbine blade.

ACKNOWLEDGEMENT

The authors would like to acknowledge the financial support received from Royal Academy of Engineering Newton Research Collaboration Programme (NRCP/1415/91) and Royal Society – China Natural Science Foundation International Exchange Award (IE150600).

REFERENCES

1. Puttock, M., “Large-scale Metrology,” CIRP Annals – Manufacturing Technology, vol. 21, no. 3, pp.351-356, 1978.
2. Estler, W., Edmundon, K. Peggs, G. and DH, P. “Large-scale Metrology – An Update,” CIRP Annals – Manufacturing Technology, vol.51, no.2, pp.587-609, 2002.
3. Peggs, G., Maropoulos, P., Hughes, E., Forbes, A., Robson, S., Ziebart, M. and Muralikrishnan, B., “Recent Developments in large-scale Dimensional Metrology,” Proceedings of the Institution of Mechanical Engineers, Part B: Journal of Engineering Manufacture, vol. 223, no. 6, pp. 571-595, 2009.
4. Franceschini, F., Galetto, M., Maisano, D. and Mastrogiacomo, L., “Large-Scale Dimensional Metrology (LSDM): from Tapes and Theodolites to Multi-Sensor Systems,” International Journal of Precision Engineering and Manufacturing, vol. 15, no. 8, pp. 1739-1758, 2014.
5. Schmitt, R. H., Peterek, M., Morse, E., Knapp, W., Galetto, M., Härtig, F., Goch, G., Hughes, B., Forbes, A., Estler, W. T. “Advances in Large-scale Metrology – Review and Future Trends,” CIRP Annals – Manufacturing Technology, vol.65, pp.643-665, 2016.
6. Wang, Q., Zissler, N., and Holden, R., “Evaluate Error Sources and Uncertainty in Large Scale Measurement Systems,” Robotics and Computer-Integrated Manufacturing, vol. 29, pp. 1-11, 2013.
7. Weckenmann, A., Jiang, X., Sommer, K-D., Neuschaefer-Rube, U., Seewig, J., Shaw, L., Estler, T., “Multisensor Data Fusion in Dimensional Metrology,” CIRP Annals – Manufacturing Technology, vol.58, pp.701-721, 2009.
8. Galetto, M. and Pralio, B., “Optimal Sensor Positioning for Large Scale Metrology Applications,” Precision Engineering, vol. 34, pp.563-577, 2010.
9. Ramasamy, S. K. and Raja, J., “Performance Evaluation of Multi-scale Data Fusion Methods for Surface Metrology Domain,” Journal of Manufacturing Systems, vol.32, pp.514-522, 2013.
10. Galetto, M., Mastrogiacomo, L., Maisano, D. and Franceschini, F., “Cooperative Fusion of Distributed Multi-sensor LVM (Large Volume Metrology) systems,” CIRP Annals – Manufacturing Technology, vol.64, pp.483-486, 2015.
11. Maisano, D. and Mastrogiacomo. L., “A New Methodology to Design Multi-sensor Networks for Distributed Large-volume Metrology Systems Based on Triangulation,” Precision Engineering, vol.43, pp.105-118, 2016.
12. Franceschini, F., Galetto, M., Maisano, D. and Mastrogiacomo, L., “Combing Multiple Large Volume Metrology Systems: Competitive Versus Cooperative Data Fusion,” Precision Engineering, vol 43, pp514-524, 2016.
13. Galetto, M., Mastrogiacomo, L., Maisano, D., Fraanceschini, F., “Uncertainty Evaluation of Distributed Large-scale-metrology Systems by a Monte Carlo Approach” CIRP Annals – Manufacturing Technology, vol.65, pp.491-494, 2016.
14. Jang, Y-S., Kim, S-W., “Compensation of the refractive Index of Air in Laser Interferometer for Distance Measurement: A Review,” International Journal of Precision Engineering and Manufacturing, Vol. 18, No. 12, pp.1881-1890, 2017.
15. Wang, J., Pagani, L., Leach, R. K., Zeng, W. H., Colosimo, B. M., Zhou, P. L., “Study of Weighted Fusion Methods for the Measurement of Surface Geometry,” Precision Engineering, vol. 47, pp.111-121, 2017.
16. Ren, M. J., Sun, L. J., Liu, M. Y., Cheung, C. F., Yin, Y. H., Cao, Y. L. “A Weighted Least Square Based Data Fusion Method for Precision Measurement of Freeform Surfaces,” Precision Engineering, vol. 48, pp.144-151, 2017.
17. Schwenke, H., Neuschaefer-Rube, U., Pfeifer, T., and Kunzmann, H., “Optical Methods for Dimensional Metrology in Production Engineering,” CIRP Annals - Manufacturing Technology, vol. 51, no. 2, pp. 685-699, 2002.
18. Savio, E. De Chiffre, L. and Schmitt, R. “Metrology of Freeform Shaped parts,” CIRP Annals - Manufacturing Technology, vol. 56, no. 2, pp. 810-835, 2007.
19. Talbot, J., Wang, Q., Brady, N., and Holden, R., “Offshore Wind Turbine Blades Measurement using Coherent Laser Radar,” Measurement, Vol. 79, pp.53-65, 2016.

DOI: XXX-XXX-XXXX

20. Summers, A., Wang, Q., Brady, N., and Holden, R. “Investigating the Measurement of Offshore Wind Turbine Blades using Coherent Laser Radar,” Robotics and Computer-Integrated Manufacturing, Vol. 41, pp.43-52, 2016.

21. Auger, D., Wang, Q., Trevelyan, J., Huang, S. L., Zhao, W. “Investigating the Quality Inspection Process of Offshore Wind Turbine Blades using B-spline Surfaces,” Measurement, Vol. 115, pp.162-172, 2018.

22. Slotwinski, A. R., Goodwin, F. E., and Simonson, D. L., “Utilizing GaalAs Laser Diodes As A Source For Frequency Modulated Continuous Wave (FMCW) Coherent Laser Radar,” Proc. SPIE, Laser Diode Technology and Applications, vol. 1043, pp. 245-251, 1989.

23. Nikon Metrology, “Laser Radar MV330/350 - For Automated, Non-contact Large Scale Metrology,” Nikon Metrology, 2014. [Online].Available: http://www.nikonmetrology.com/en_EU/Products/Large-Volume-Applications/Laser-Radar/MV330-MV350-Laser-Radar. [Accessed July 2018].

24. New River Kinematics, “Spatial Analyzer,” New River Kinematics, 2014. [Online]. Available: http://www.kinematics.com/spatialanalyzer/. [Accessed July 2018].

25. de Boor, C., “On Calculating with B-splines,” Journal of Approximation Theory, vol. 6, no. 1, pp. 50-62, 1972.

26. Tai, C., Hu, S., and Huang, Q., “Approximate Merging of B-spline Curves via Knot Adjustment and Constrained Optimization,” Computer-Aided Design, vol. 35, pp. 893-899, 2003.

27. Chen, X., Ma, W., Xu, G., and Paul, J.-C, “Computing the Hausdorff Distance between two B-spline Curves,” Computer-Aided Design, vol. 42, no. 12, pp. 1197-1206, 2010.

28. Yang, Y., Cao, S., Yong, J., Zhang, H., Paul, J.-C. J., Sun, J., and Gu, H., “Approximate Computation of Curves on B-Spline Surfaces,” Computer-Aided Design, vol. 20, no. 2, pp. 223-234, 2008.

29. Yang, H., Wang, W., and Sun, J., “Control Point Adjustment for B-Spline Curve Approximation,” Computer-Aided Design, vol. 36, pp. 639-652, 2004.

30. Li, H., and Kong, X., “A Novel Modeling Approach in Blade Shape Design,” Journal of Convergence Information Technology, vol. 8, no. 8, pp. 1013-1020, 2013.